Physics – Uspekhi **60** (10) 1039 – 1050 (2017)

CONFERENCES AND SYMPOSIA

PACS numbers: **29.20. – c**, 29.27.Ac, 42.60.By, **42.60. – v**

Spatio-temporal shaping of photocathode laser pulses for linear electron accelerators

S Yu Mironov, A V Andrianov, E I Gacheva, V V Zelenogorskii, A K Potemkin, E A Khazanov, P Boonpornprasert, M Gross, J Good, I Isaev, D Kalantaryan, T Kozak, M Krasilnikov, H Qian, X Li, O Lishilin, D Melkumyan, A Oppelt, Y Renier, T Rublack, M Felber, H Huck, Y Chen, F Stephan

DOI: https://doi.org/10.3367/UFNe.2017.03.038143

Contents

Abstract. Methods for the spatio-temporal shaping of photocathode laser pulses for generating high brightness electron beams in modern linear accelerators are discussed. The possibility of forming triangular laser pulses and quasi-ellipsoidal structures is analyzed. The proposed setup for generating shaped laser pulses was realised at the Institute of Applied Physics (IAP) of the Russian Academy of Sciences (RAS). Currently, a prototype of the pulse-shaping laser system is installed at the Photo Injector Test facility at DESY, Zeuthen site (PITZ). Preliminary experiments on electron beam generation using ultraviolet laser pulses from this system were carried out at PITZ, in which electron bunches with a 0.5-nC charge and a transverse normalized emittance of 1.1 mm mrad were obtained. A new scheme for the three-dimensional shaping of laser beams using a volume Bragg profiled grating is proposed at IAP RAS and is currently being tested for further electron beam generation experiments at the PITZ photoinjector.

Keywords: 3D-shaping of laser pulses, photoinjector, linear electron accelerator, generation and acceleration of electron beams, normalized transverse emittance

S Yu Mironov, A V Andrianov, E I Gacheva, V V Zelenogorskii, A K Potemkin, E A Khazanov Institute of Applied Physics, Russian Academy of Sciences, ul. Ul'yanova 46, 603950 Nizhny Novgorod, Russian Federation
P Boonpornprasert, M Gross, J Good, I Isaev, D Kalantaryan, M Krasilnikov, H Qian, X Li, O Lishilin, D Melkumyan, A Oppelt, Y Renier, T Rublack, H Huck, Y Chen, F Stephan Deutsches Elektronen-Synchrotron, Platanenallee 6, Zeuthen, D-15738, Germany
T Kozak, M Felber Deutsches Elektronen-Synchrotron, Notkestrasse 85, Hamburg, D-22603, Germany
E-mail: Sergei.Mironov@mail.ru, alex.v.andrianov@gmail.com, gacheva@appl.sci-nnov.ru, vvmailv@mail.ru, ptmk@appl.sci-nnov.ru, khazanov@appl.sci-nnov.ru, mikhail.krasilnikov@desy.de, frank.stephan@desy.de

Received 16 May 2017
Uspekhi Fizicheskikh Nauk **187** (10) 1121 – 1133 (2017)
DOI: https://doi.org/10.3367/UFNr.2017.03.038143
Translated by A L Chekhov; edited by A Radzig

1. Introduction

Currently, one of the most important fields utilizing methods for three-dimensional laser pulse shaping is related to electron photoinjector physics. Here, laser pulses are employed to illuminate a photocathode surface in order to generate electron bunches resulted from a photoeffect. The cathode is placed in a vacuum chamber inside a microwave cavity. The laser pulse repetition rate is a subharmonic of a microwave field, which allows generating synchronized with the microwave device laser pulses and efficiently accelerating generated electron bunches.

It is well known that the intensity distribution of laser pulses determines the electron beam parameters, such as the spatial distribution of the charge, the value of the transverse normalized emittance, and others. By controling the spatio–temporal distribution of the laser pulse intensity one can change the electron bunch parameters. The required electron beam characteristics are defined by the specific tasks for which they are generated.

One of the most promising applications is the development of free-electron lasers (FELs) operating in the single-pass self-amplified spontaneous emission (SASE) mode. In this case, electron bunches should satisfy strict requirements for the peak brightness and stability, so one needs to generate very short electron bunches with high current (on the order of

several kiloamperes) and very small transverse emittance (~ 1 mm mrad). The emission of electron bunches with similar properties is complicated due to the significant influence of Coulombic repulsion forces. Therefore, in modern linear accelerators a system with subsequent compression of the electron beam (for example, in a magnetic bunch-compressor) is exploited. Since the dynamics of electron beams in a linear accelerator imply only an increase in the transverse phase volume (normalized emittance), the generation of electron bunches with small (< 1 mm mrad) emittance in the injector is a necessary condition for the efficient operation of FELs. Picosecond laser pulses (1 – 30 ps) are used in modern photoinjectors in order to reduce the influence of the spatial charge forces in electron beams with the characteristic charge of ~ 1 nC and energy of 5 – 7 MeV.

Currently, experiments on the generation of such electron bunches are performed at the world's biggest accelerator facilities: in Germany at the Deutsches Elektronen-Synchrotron (DESY), which has sites in Hamburg (free-electron laser in Hamburg, FLASH) and in Zeuthen (PITZ photoinjector), in Japan at the High Energy Accelerator Research Organization (KEK), in Russia at the Joint Institute for Nuclear Research (JINR, Dubna) and at the IAP RAS (Nizhny Novgorod), and in the USA at the Argonne National Laboratory and the SLAC National Accelerator Laboratory.

Another feature of modern FELs consists in their capacity to form a sequence (train, packet) of micropulses, which is a necessary condition for the realization of many experiments with FEL radiation and for the significant improvement of statistical sampling of the measurements. For example, the European X-ray FEL (European XFEL) can generate a train of 2700 micropulses (time interval between the pulses in the train is 222 ns) with a 10-Hz repetition rate.

As an example, we will review the most interesting latest results on the generation of electron bunches with laser pulses. At the FLASH photoinjector, 10-ps Gaussian laser pulses generated electron bunches with 1-nC charge, 2.1-mm mrad emittance, and 100-MeV energy [1]. At the PITZ photoinjector, 21.5-ps flattop laser pulses (quasi-cylindrical beams) with 2-ps rising edges [2] generated electron bunches with a record-small normalized emittance of 0.7 mm mrad for a 1-nC bunch charge [3].

In 1959, it was reported in paper [4] that a uniformly filled elliptical transverse phase distribution of a beam corresponds to a minimal normalized emittance. Such a distribution is called a Kapchinskij–Vladimirskij distribution. The main advantage of such a distribution is that the Coulomb repulsive forces of the spatial charge are linear and can be compensated for by means of electron optics. Numerical simulations have shown that generalizing this distribution to the three-dimensional (3D) case (ellipsoid) corresponds to a significant reduction in beam emittance. Thus far, trains of such electron bunches have not been generated in experiments.

The first step towards the formation of ellipsoidal electron bunches is the generation of correspondingly shaped laser pulses used for electron photoemission. In these pulses, the intensity distribution is uniform inside the ellipsoidal volume, and is zero outside of it. To date, however, there have been no experimentally realizable methods for the formation of ellipsoidal structures in laser pulses. It is important to note that, from the experimental point of view, generating such laser pulses is impossible due to the infinite value of the field derivative at the boundary. In fact, the limitation is connected with the infinite spatial and temporal spectrum. Hence, we will further describe the electric field of such laser pulses with a suitable smooth function, super-Gaussian, for example, and the corresponding distribution will be named quasi-ellipsoidal.

Most modern investigations concerned with laser pulse shaping deal with control over the laser intensity distribution either in time or in space. Examples of full 3D shaping are presented in a few pioneering studies. For example, ultraviolet cylindrical beams were obtained in paper [2] by using independent consequent shaping in time and space. The method is based on the Solc birefringent filter. Temporal shaping was performed using 10 uniaxial crystals rotated with respect to each other. The difference between group velocities of ordinary and extraordinary waves allows realizing one-dimensional shaping.

It should be noted that cylindrical pulses have already resulted in a significant increase in emittance with respect to that obtained by injection of a nonshaped (Gaussian) beam. The authors of paper [5] suggested a very original, but not universal, approach to quasiellipsoidal beam formation based on a Dazzler device of the French company Faslite and a lens with significant chromatic aberrations; the 3D ellipsoidal structure in this case is formed in the far-field zone. It was suggested in paper [6] that an ellipsoidal electron beam be created after the injection stage in the so-called blowout regime. In this case, the cathode should be illuminated with an ultrashort laser pulse and the electric field during the emission process should reach quite large amplitudes (> 100 MV m^{-1} for practical values of the beam charge).

The considered approaches have fundamental limitations over the pulse energy and cannot be applied to generating electron bunches with a charge of ~ 1 nC, which requires developing alternative approaches. One promising method for spatio–temporal control over the intensity distribution is based on utilizing spectrons — pulses with a significant linear frequency modulation [7]. When the pulse length is significantly larger than its Fourier limit, control over the frequency spectrum shape corresponds to control over the intensity distribution in time. Thus, in order to generate cylindrical pulses, one needs to obtain a rectangular distribution of the frequency spectrum and quasiflat transverse intensity distribution. This problem was successfully solved in Ref. [8] by using programmable spatial light modulators (SLMs). The experiment resulted in the generation of 42-ps long cylindrical pulses. An original method for the formation of quasi-ellipsoidal laser pulses was demonstrated in the same study. The pulses demonstrate 90° axial symmetry and are ellipses in two mutually orthogonal longitudinal cross sections.

In paper [9], it was suggested that a profiled volume chirped Bragg grating be used in order to form 3D-ellipsoidal pulses from cylindrical ones. To the best of our knowledge, this is the first successful experimental realization of 3D-ellipsoidal pulses with axial symmetry. The pulse length was 264 ps.

In the present paper, we discuss the features of the currently operating linear electron accelerator PITZ and of the laser system built for it with the capacity to generate shaped pulses in the ultraviolet region. We analyze the method for generating ultrashort (several picoseconds long) ellipsoidal pulses using a profiled Bragg grating and a programmable SLM, and present the results on electron bunch generation at the PITZ accelerator. An approach to

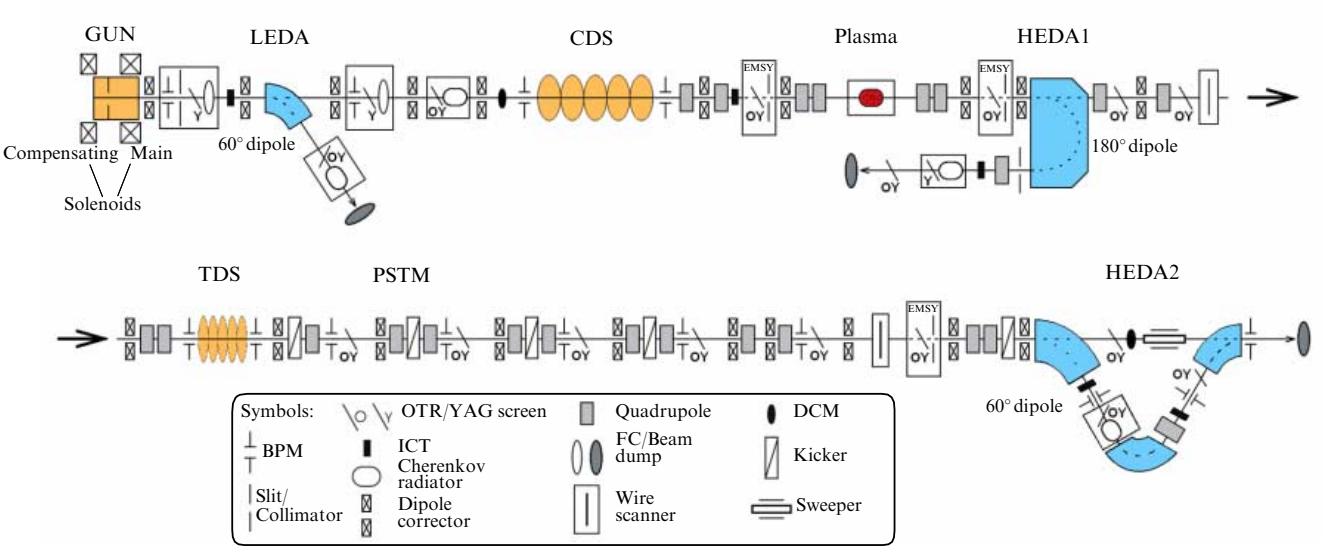

Figure 1. PITZ linear accelerator schematic: GUN — microwave photogun, CDS — cut disk structure or linear accelerating section (booster), TDS — microwave transverse deflecting system, LEDA — low energy dispersive arm, and HEDA1, 2 (high-energy dispersive arms) — dipole magnets for the measurement of electron bunch longitudinal moment, PSTM (phase space tomography module) — periodical system of quadrupole magnets for the tomography of electron beam transverse phase space, Plasma — removable plasma section for the investigation of plasma wake acceleration, EMSY — emittance measurement system, BPM — beam position monitor, ICT — integrating current transformer (Rogowski coil), OTR — optical transition radiation screen, and DCM — dark current monitor.

forming axially symmetric quasiellipsoidal structures with linearly increasing intensity from the pulse front edge to its 'tail' is described, and experimental results on the generation of triangular pulses are presented.

2. Generation of high-brightness electron beams in modern photoinjectors

2.1 PITZ linear accelerator

Since the moment of its conception, the PITZ photoinjector was intended to develop and optimize high-brightness electron beam sources for modern FELs, in particular, for user setups based on superconducting linear accelerators. The choice of photoinjector technology is dictated by strict requirements on the electron beam properties — large phase volume density under high stability and the on-off time ratio. A general schematic of the PITZ linear accelerator is presented in Fig. 1.

The electron source for the PITZ photoinjector is a microwave photogun based on an accelerating section with $1^1/_2$ cells and two magnetic (solenoid) lenses for the compensation of transverse emittance. A 10-megawatt klystron with an average frequency of 1.3 GHz provides a standing wave in the gun accelerating section with peak power corresponding to the maximum strength of the electric field on the photocathode surface on the order of 60 MV m^{-1}, which results in a maximum electron acceleration up to 6.5 MeV. Further acceleration of electron bunches up to energies of 20 – 25 MeV is performed in a CDS booster. The high quantum efficiency of the Cs_2Te photocathode ($\sim 5-10\%$), located in the center of the microwave gun backplane, provides the generation of electron beams with a high charge (up to 5 nC). The beams that follow with a 1-MHz repetition rate are grouped in trains of up to 600 pulses, the train repetition rate being 10 Hz. Such a temporal structure is provided by the corresponding grouping of photocathode laser pulses.

The main laser system currently used at PITZ was developed at the Max-Born-Institut in Berlin. This system already provides the possibility of producing temporally rectangular laser pulses: the longitudinal distribution of pulse intensity can be varied from Gaussian (FWHM $\sim$ 11.5 ps) to flattop (20 – 22 ps FWHM with 2-ps edges) [2].

The results of experimental optimization of transverse normalized emittance are given in Fig. 2 as functions of beam charge compared to corresponding beam dynamics calculations. Simulations were performed using the ASTRA program code [10]. Blue curves correspond to nominal parameters of the European XFEL photoinjector: 60.6 MV m^{-1} electrical microwave field strength at the cathode and flattop laser pulses. Red curves correspond to the starting parameters of the same setup: 53-MV m^{-1} field amplitude and Gaussian profile (11.5-ps FWHM) of the photocathode laser pulse.

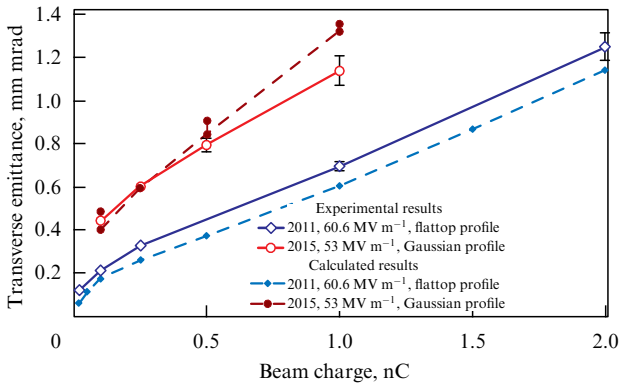

Figure 2. (Color online.) Measured (solid curves) and calculated (dashed curves) normalized emittance versus beam charge. Red curves correspond to microwave field amplitude of 60.6 MV m^{-1} at the cathode and flattop photocathode pulses with a 21.5-ps duration (FWHM) and approximately 2-ps edges. Blue curves correspond to the lower field at the cathode (53 MV m^{-1}) and Gaussian laser pulses with an 11.5-ps duration (FWHM).

Table 1. Parameters of numerical calculations for PITZ photoinjector using different photocathode laser pulse profiles: cylindrical pulse with Gaussian and flattop temporal distributions, and an ellipsoidal pulse.

Conditions and parameters		Three-dimensional structure		
		Cylinder		Elipsoid
		Gaussian longitudinal profile	Flattop longitudinal profile	Uniformly filled
Photo-cathode laser	Pulse length (FWHM)	9.5 ps		
	Transverse distribution	Uniform radial distribution		Uniform distribution
	Root-mean-square (rms) lateral dimension	0.385 mm	0.423 mm	0.353 mm
Microwave gun	Electric field at the cathode	60 MV m^{-1}		
	Phase*	−1.2°	−4.2°	−2.8°
	Solenoid field (maximal)	−0.2247 T	−0.2248 T	−0.2260 T
Booster	Electric field (maximal)	17.1 MV m^{-1}		
	Phase*	0		
Electron beam ($z = 5.277$ m)	Charge	0.5 nC		
	Mean kinetic energy	21.0 MeV	21.0 MeV	21.0 MeV
	Normalized transverse emittance (designed)	0.80 mm mrad	0.64 mm mrad	0.35 mm mrad
	Slice transverse emittance	0.49 mm mrad	0.57 mm mrad	0.33 mm mrad
	Bunch length (rms)	1.44 mm	1.20 mm	1.34 mm
	Beam peak current	35.4 A	39.5 A	37.8 A
	Beam longitudinal emittance	34 mm keV	22 mm keV	12.5 mm keV

* Relative to phase of the maximum beam energy gain.

These experimental curves are also compared with numerical calculation results. The data shown in Fig. 2 evidently demonstrates the importance of photocathode laser pulse shaping and the need to achieve high electric field strengths at the photocathode.

2.2 Numerical optimization of PITZ photoinjector for various shapes of laser pulses

From a comparison of emittance curves for different photocathode laser pulse shapes (see Fig. 2), it can be seen that the transition from a Gaussian longitudinal profile to a flattop longitudinal profile leads to a significant decrease in the transverse emittance for the whole range of beam charges. In the case shown in Fig. 2, however, the measurements (and the corresponding calculations) were performed for different electric field strengths at the photocathode, which also influences the electron source brightness, so it is hard to filter out the 'pure' influence of only the pulse shape on the emittance. Therefore, numerical simulations of beam dynamics were performed for various shapes of photocathode laser pulses with a fixed electric field amplitude. The results of these calculations are given below.

It is known that the main reason for the increase in the transverse emittance of electron photoinjector beams is the Coulomb repulsive forces of the spatial charge. The nonlinear character of these forces leads to nonlinear distortions of the transverse phase space and to an increase in emittance. It is also known that the field of a charge evenly distributed inside an ellipsoid is linear and, thus, does not result in nonlinear distortions of the phase space. This fact motivated the development of a laser system for the generation of ellipsoidal electron beams by correspondingly shaping the laser pulses. Calculations for different laser pulse profiles in PITZ photoinjector were performed using the ASTRA code [10] with parameters shown in Table 1. In the same table, we collate them with the optimization results for the transverse normalized emittance of the electron beam.

Three characteristic photocathode laser pulse profiles were invoked in the calculations (Fig. 3): two cylindrical profiles with Gaussian and flattop temporal distributions, and a three-dimensional profile with an ellipsoidal uniform intensity distribution. Numerical optimization of the normalized emittance was performed for a beam with a

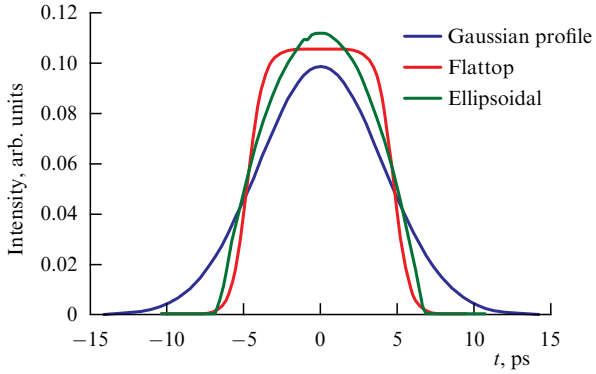

Figure 3. (Color online.) Longitudinal profiles of laser pulses used in numerical simulations.

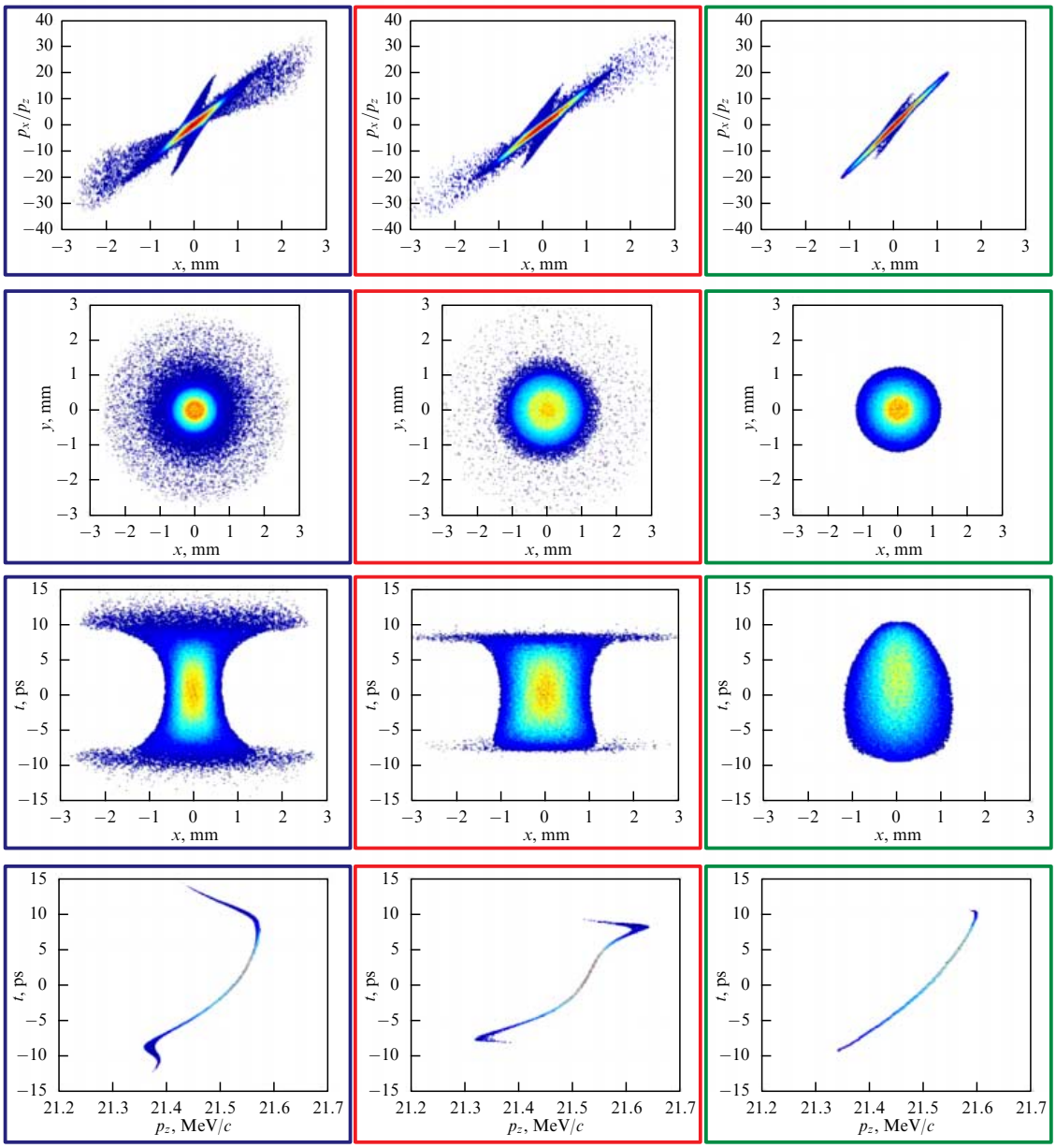

Figure 4. Results of numerical optimization of the electron beam transverse emittance for Gaussian (left column), flattop (central column), and ellipsoidal (right column) laser pulses. First row — transverse (horizontal, $x-p_x$) phase space, 2nd row — transverse $x-y$-distribution, 3rd row — side $x-t$-projection, and 4th row — longitudinal (p_z-t) phase space of the electron beam.

0.5-nC charge positioned in a linear accelerator at the point of 5.277 m, where the transverse phase space was measured. The pulse length of the photocathode laser was chosen close to the experimental values from the measurements presented in this article. Emittance minimization was performed by varying the main parameters of the photoinjector: the main solenoid current, the lateral size of the laser beam at the cathode, and the initial phase of the microwave gun. Other parameters had nominal PITZ experimental values.

Optimization results are shown in Table 1 and in Fig. 4, where normalized emittances are shown together with transverse and longitudinal phase spaces and electron beam profiles.

Of specific interest is the phase distribution along the electron beam. Slice emittance is shown in Fig. 5 together with the beam current profile for three different profiles of photocathode laser pulses. By comparing slice emittances, one can see a significant reduction in the electron beam slice phase volume in the case of ellipsoidal laser pulses. It is evident that by using ellipsoidal laser pulses the electron beam properties can be significantly improved: there is a reduction in transverse and longitudinal halos and a lower nonlinearity of the longitudinal phase space. Preliminary analysis of the electron beam shape, generated by ellipsoidal laser pulses, shows that due to the action of the space charge (including the forces resulting from the image charge during photoemission) the ellipsoidal shape of the initial beam is distorted. Therefore, the photoinjector may be further optimized by correspondingly deforming the laser pulse in order to generate an electron ellipsoid.

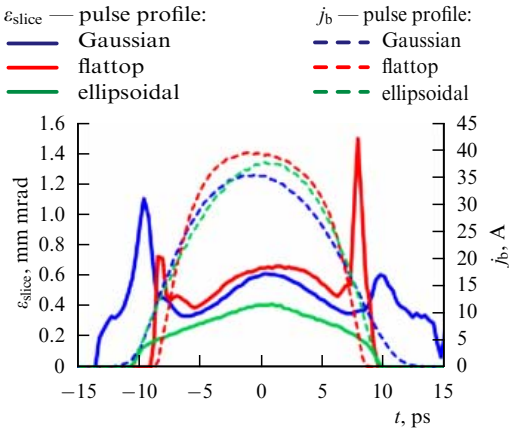

Figure 5. (Color online.) Slice emittance ε_{slice} of optimized electron bunches for various profiles of photocathode pulses (solid curves). Corresponding beam current j_b profiles (dashed lines) correspond to the right-hand y-axis.

3. Three-dimensional shaping of laser pulses

3.1 Photocathode laser at PITZ linear electron accelerator

Laser system includes a fiber laser, a diode-pumped disk Yb:KGW-amplifier,[1] a spatio–temporal shaper, second harmonic (SHG) and fourth harmonic (FHG) generators, and a system to measure the radiation parameters. A general schematic is shown in Fig. 6. The fiber section includes a master oscillator (MO), which generates 200-fs pulses with a 27-MHz repetition rate, a fiber stretcher, a preamplifier, a system for macropulse formation, a radiation splitter into operating and diagnostic channels, and two wide-aperture fiber amplifiers. The MO fiber is wound onto a piezoceramic cylinder for precise tuning of the laser pulse repetition rate to the closest subharmonic of the klystron frequency.

The operating channel of the laser further amplifies the radiation, spatio–temporally shapes the pulses, and generates their optical harmonics (second and fourth). Diagnostic channel radiation is used in a cross-correlator to measure spatio–temporal characteristics of the operating channel output radiation. Inside the cross-correlator crystal, diagnostic channel pulses and IR/UV-shaped pulses interact nonlinearly (second/third harmonic generation). The length of the diagnostic channel pulses is close to its Fourier limit: ≈ 200 fs. The length of the operating channel pulses is ≈ 20 ps. In this case, the measured signal is proportional to the intensity distribution inside the shaped pulse. Measurements are performed using either a fast CCD-camera (charge-coupled device) or a photodiode. The variable delay line used for fast temporal scanning is made by winding an 80-m section of the diagnostic channel fiber onto another piezoceramic disc [11].

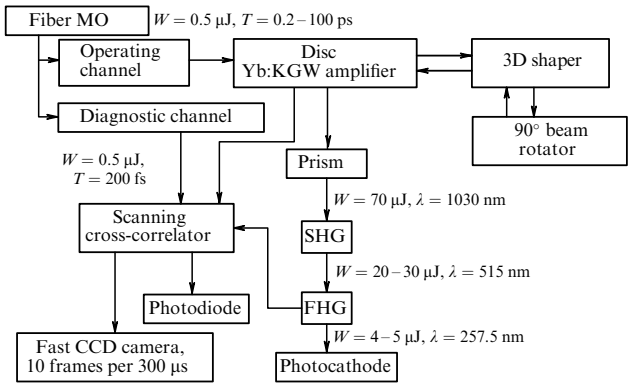

Figure 6. Schematic of the laser at the PITZ DESY linear accelerator.

[1] KGW — Potassium–gadolinium tungstate.

Operating channel radiation is amplified in a multipass disc amplifier with Yb:KGW crystals as active elements (AEs). There are two active elements — quantrons — in the amplifier. The signal makes five V-passes around the first AE, and four V-passes around the second one. The surface image of the first AE is transferred to the surface of the second one without scaling. The mirrors are mounted in such a way that after every reflection from the AE the laser beam shifts along the surface of the mirrors and leaves the amplifier after a certain number of reflections. An astigmatism caused by oblique incidence of the beam on the spherical mirror surfaces is compensated for by the special geometry of the mirror telescope [12]. The amplifier allows increasing pulse energy from 0.5 μJ to 70 μJ in two passes.

A spatio–temporal shaper is installed between forward and backward passes of the amplifier. It forms quasi-ellipsoidal pulses with a 90° symmetry. Intensity distributions of such pulses are ellipses in both orthogonal (xt and yt) cross sections.

The pulse shaper (Fig. 7) comprises an optical compressor with zero frequency dispersion [8]. The shaper consists of two diffraction gratings, two liquid-crystal SLMs, and two 1×-magnification Kepler telescopes with cylindrical and spherical lenses. SLMs are located on the focal planes of the telescope with cylindrical lenses, which transfers the image along the longitudinal plane from one diffraction grating to another. The image is not transferred in the sagittal plane, so diffraction takes place. Image transfer from one SLM to another is realized through a telescope with spherical lenses. A half-wave plate rotates the radiation polarization by 45° in front of the second SLM. The SLM introduces a voltage-controlled phase difference between orthogonal polarizations. The polarizer and the above-mentioned half-wave plate allow using the SLM2 in the spatio–temporal amplitude mask mode. The shaper design provides the ability to control the spectrum intensity distribution in space. Let us recall that the operating channel pulses are significantly chirped. In this case, control over the spectral intensity corresponds to that over the temporal distribution of the intensity. More detailed information about the shaper operation and experimental results on the generation of quasiellipsoidal pulses can be found in paper [8].

After 3D shaping, the radiation is directed to nonlinear crystals, where it is subsequently transformed into second and fourth harmonics. In order to increase the conversion efficiency and maintain the 3D distribution of the intensity, laser pulses are provided with an angular chirp. The size of the chirp is calculated in such a way that every spectral component propagates in the nonlinear crystal under an optimal angle with respect to the optical axis. Angular chirp can be introduced by a prism or a diffraction grating. We utilized a prism. The chirp magnitude can be controlled by the Kepler telescopes.

After frequency conversion, the ultraviolet radiation is directed through a transportation line to the injector photo-

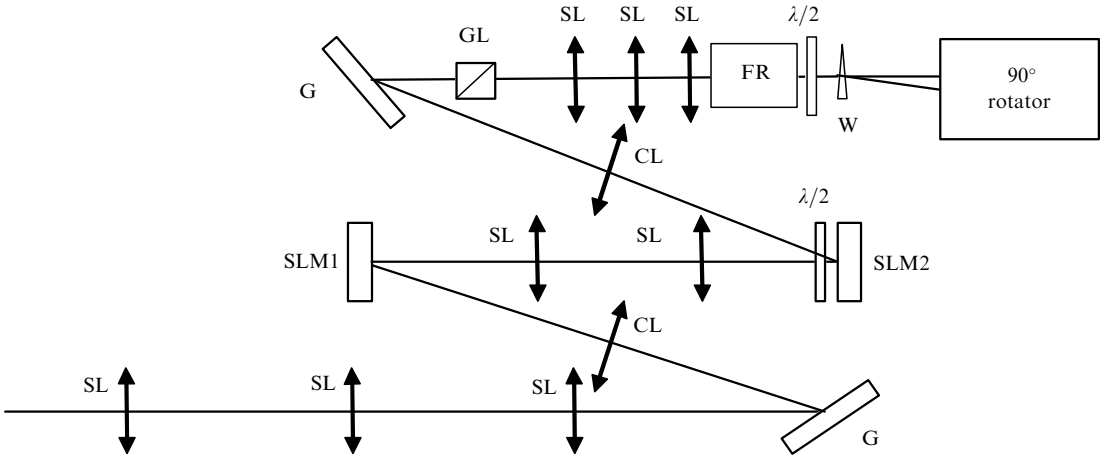

Figure 7. General schematic of the shaper for pulses with 90° axial symmetry: SL — spherical lens, CL — cylindrical lens, G — diffraction grating, SLM — spatial light modulator, FR — 45° Faraday rotator, W — calcite wedge, GL — Glan prism, and $\lambda/2$ — half-wave plate.

cathode. Ahead of the transportation line, a part of the radiation is sent to the cross-correlator for diagnostics. Let us also note that image transfer is realized both in the laser system and in the transportation line, so the shaped laser pulses are correctly transported.

3.2 Controling the pulse shape using a profiled, chirped volume Bragg grating

In a number of tasks connected with generating electron bunches on the photocathode surface, 3D ellipsoidal pulses with a duration of only several picoseconds must be used. Requirements for the pulse edges and the deviation of 3D intensity distribution profile from an ideal ellipsoid are defined by the necessary characteristics of the electron beams.

A universal method for the formation of ellipsoidal pulses using an SLM and a profiled volume Bragg grating was proposed and experimentally confirmed in paper [9]. A cylindrical pulse is directed to a volume Bragg grating recorded inside an ellipsoidal volume and absent outside it. The grating is recorded in the bulk of a photothermorefractive glass [13]. The cylindrical pulse, which is formed using the SLM-based spatio–temporal shaper [8, 9], usually exhibits linear frequency modulation. After reflecting from a spatially profiled Bragg grating, the pulse transforms into an ellipsoidal one (Fig. 8).

During the shaping of the pulse with cylindrical spatial intensity distribution using the SLM-based scheme, one can control both the edges and the shape. If a spectral mask with more sharp edges is applied to a chirped Gaussian pulse with a fixed length, it will cut a quasirectangular spectrum out of the Gaussian one, which will result not only in sharper edges in the time domain, but also in larger modulation of the longitudinal (temporal) intensity distribution [8]. If the initial Gaussian pulse experiences strictly linear frequency modulation, then, by increasing its length with respect to its Fourier limit before the application of the spectral mask, the modulation in the time domain can be reduced.

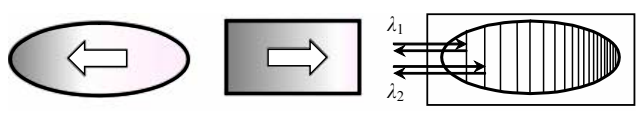

Figure 8. General schematic for 3D-ellipsoidal pulse formation using a profiled volume Bragg grating.

Cylindrical pulse formation is only the necessary first step on the way to the generation of 3D-ellipsoidal structures. The profiled Bragg grating not only shapes the spectrum intensity distribution in space, but also changes the phase of the frequency spectrum and, consequently, the pulse length. Pulse length can be controlled by changing the frequency chirp in the initial cylindrical pulse. This can be realized by using either an optical compressor or another Bragg grating without a spatial profile, but with a reverse order of reflective layers. Key parameters of the Bragg grating are the spectral reflection band and the introduced frequency chirp.

As an example, let us consider the possibility of generating 7-ps long 3D-ellipsoidal infrared pulses in IR spectral region from laser pulses with a Gaussian spectrum centered at 1030 nm and with FWHM $\Delta\Omega = 22$ nm. Notice that, from the mathematical point of view, the Gaussian spectrum contains a rectangular spectrum with any given width; however, the energy stored in this spectrum can be extremely small. The optimal width of a rectangle 2Λ inscribed in a Gaussian distribution function can be related to $\Delta\Omega$ in the following way [8]:

$$2\Lambda = \frac{\Delta\Omega}{\sqrt{2\ln 2}}\,.$$

In this case, the efficiency reaches 48%. By applying a two-dimensional amplitude mask to the transversal intensity distribution, one can transform the Gaussian profile into the rectangular one (Fig. 9).

Three-dimensional intensity distribution over time and space is illustrated in Fig. 10. The duration of the reported ellipsoid amounts to 7.4 ps, and the edge length is 1.6 ps.

A structure similar to the 3D intensity distribution was obtained in experiments performed at IAP RAS [9]. An example of the experimental distribution is given in Fig. 11.

3.3 Experimental generation of quasitriangular pulses

Over the last few years, one of the methods of electron acceleration has become quite popular. Electrons are accelerated in a wake wave field, which is generated in a periodical waveguiding structure, when a high-power electron beam with a large charge passes through it. The highest efficiency can be achieved when the initial beam charge distribution is

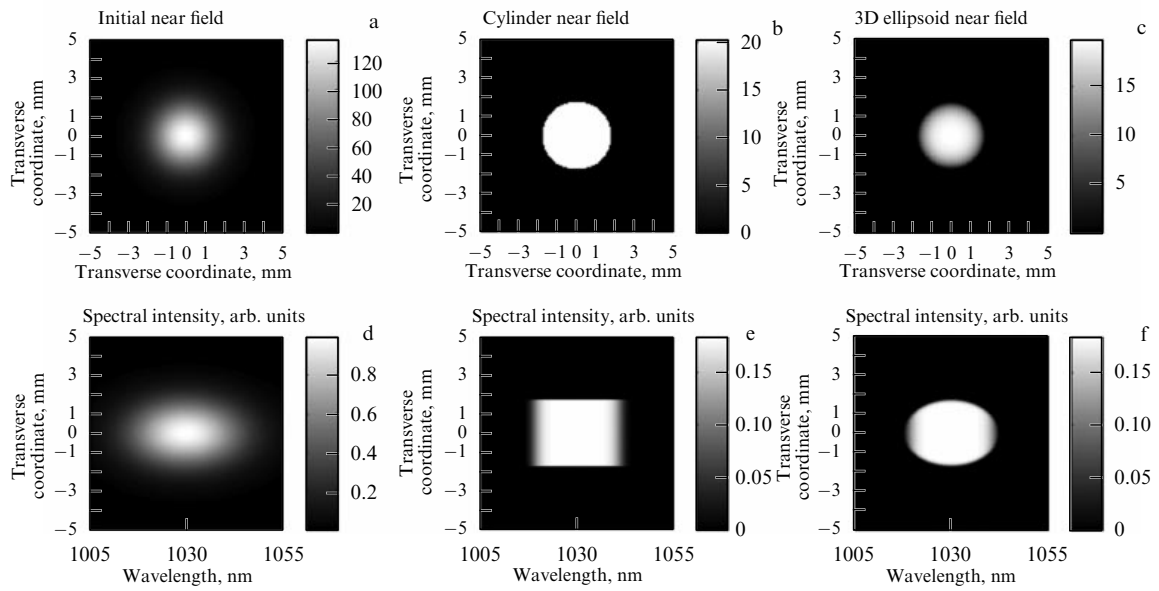

Figure 9. Transformation of a 3D Gaussian pulse into a cylindrical pulse and 3D-ellipsoidal pulse. (a–c) Transformation sequence from Gaussian near-field (initial) zone into quasihomogeneous one and into the 3D-ellipsoidal near-field zone. (d–f) Corresponding transformation of the spectral intensity.

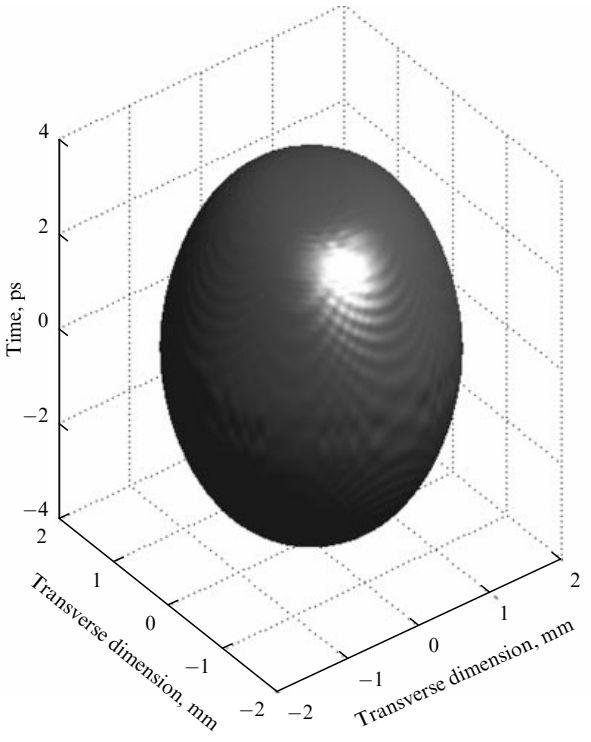

Figure 10. 3D intensity distribution of an ellipsoidal pulse.

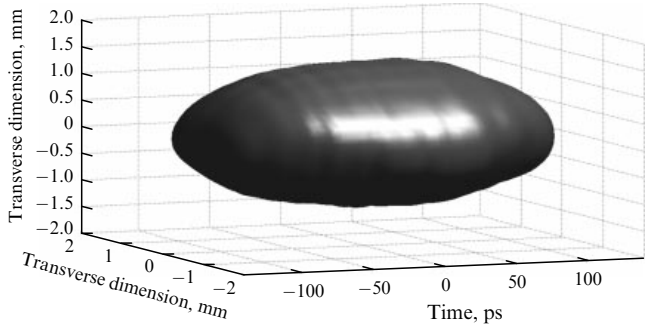

Figure 11. 3D-quasiellipsoidal intensity distribution obtained in the experiment.

triangular in time. Such beams can be produced during injection from the photocathode surface.

For these purposes, one can use a method for control over the spatio–temporal intensity distribution of laser pulses based on the spatial light modulator described above. In this case, a triangle should be filtered out from a Gaussian spectrum. If the laser pulse has a significant linear frequency modulation (the pulse length is much larger than the Fourier limit), then the intensity distribution in time will also be triangular. The triangular pulse length can be controlled in the experiment by changing either the spectral phase or the length of the spectral triangle base. The length of the triangular pulse trailing edge is determined both by the sharpness of the spectral mask applied to the Gaussian pulse during the triangular cutting and by the linear chirp strength. Experimental realization of triangular pulses is demonstrated in Fig. 12.

It is important to note that laser pulses with triangular temporal and quasirectangular spatial intensity distributions can be employed to illuminate the profiled Bragg grating. In this case, the intensity distribution will be axially symmetric and the intensity will linearly increase in time. Such pulses can be utilized to illuminate photocathodes in order to generate quasiellipsoidal bunches with a large spatial charge. The larger field in the pulse tail will allow overcoming the Coulomb attractive forces acting on the electron bunch detached from the cathode surface.

4. Generation and characterization of electron beams at PITZ photoinjector

The first experiments on electron bunch generation at PITZ applying a laser system with a controllable laser pulse

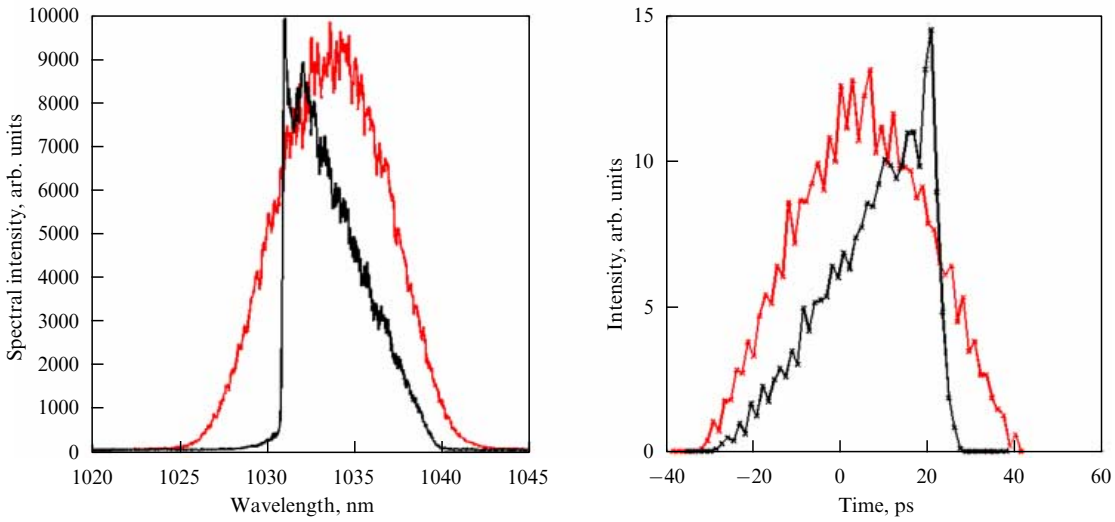

Figure 12. Generation of triangular pulses in the experiment.

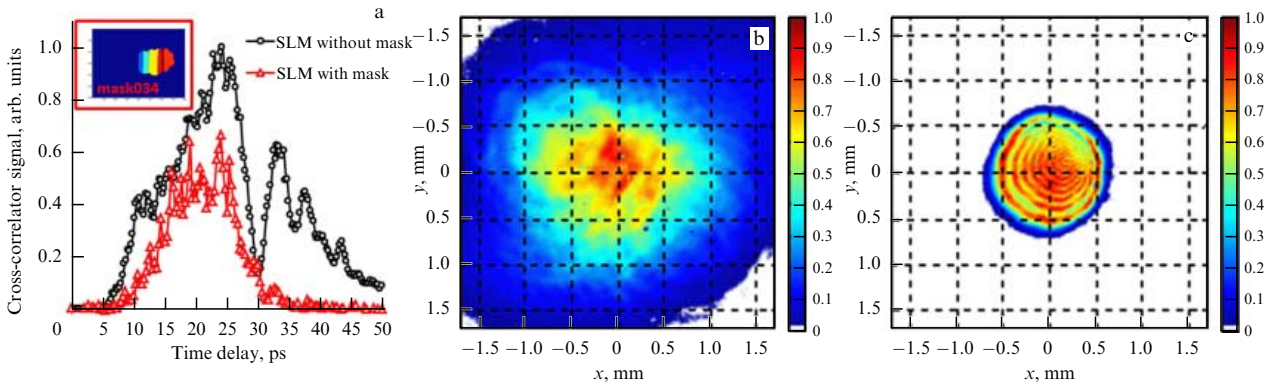

Figure 13. (Color online.) (a) Measurements of the longitudinal profile of a photocathode laser IR pulse using a cross-correlator. Transverse intensity distribution I (arb. units) of the photocathode laser: (b) for a full beam, and (c) for a beam restricted by an aperture 1.2 mm in diameter.

intensity distribution were started in December 2016. The main task was to demonstrate the possibility of standard optimization of the electron beam brightness, which implies the measurements of the transverse emittance and longitudinal profile of the electron bunches. For this cycle of experiments, the nominal beam charge was chosen to be 0.5 nC. Laser beam shaping was performed with an experimentally optimized SLM mask 034. Figure 13a plots the profiles of the infrared (IR) pulses measured using a cross-correlator with and without application of the SLM mask.

Application of the mask leads to a significant shortening of the IR pulse from 24–26 ps to 10–12 ps. Taking into account SHGs and FHGs, the UV pulse length further decreases and reaches approximately 9–10 ps, which corresponds to the input parameters of the calculations discussed in Section 2.2.

For transverse diagnostics of the laser beam, we used a CCD camera located in the plane optically equivalent to the photocathode surface plane. Examples of the beam images obtained with and without utilization of a shaping aperture 1.2 mm in diameter are shown in Figs 13b, c, respectively.

Peak powers of the microwave radiation in the microwave gun and the booster acceleration section, being 6.4 and 3 MW, respectively, were used to generate and accelerate the electron bunches. Both accelerating structures were tuned to the maximum acceleration phases. Measurement results — average longitudinal momentum $\langle p_z \rangle$ and its standard deviation p_z^{rms} — are presented in Figs 14a and 15a as functions of the gun and booster phases, respectively. Figures 14b and 15b show the particle density distribution of the beam over the longitudinal momentum p_z for nominal (zero) phases. Zero phases in both cases were chosen among those corresponding to the maximum beam energy gain in the acceleration structure. This conforms to an average longitudinal momentum $\langle p_z \rangle$ of the electron beam of 6.57 MeV/c at the gun output, and 22.3 MeV/c after accelerating in the booster. The respective standard deviations of the longitudinal momentum are 25 and 20 keV/c. Minimal longitudinal momentum deviations measured for gun phase -8° and booster phase 1° are 4.8 and 19.0 keV/c, respectively.

The energy of the photocathode laser pulse used in the experiment provided a beam charge of 0.5 nC for the zero phase of the gun (see Fig. 14) and a 1.2-mm laser beam diameter at the cathode. The charge was measured and controlled using a Rogowski coil (fabricated by Bergoz Instrumentation) located at a distance of 0.9 m from the photocathode. Typical results of the beam charge measurements under these conditions are given in Fig. 16. It is clear

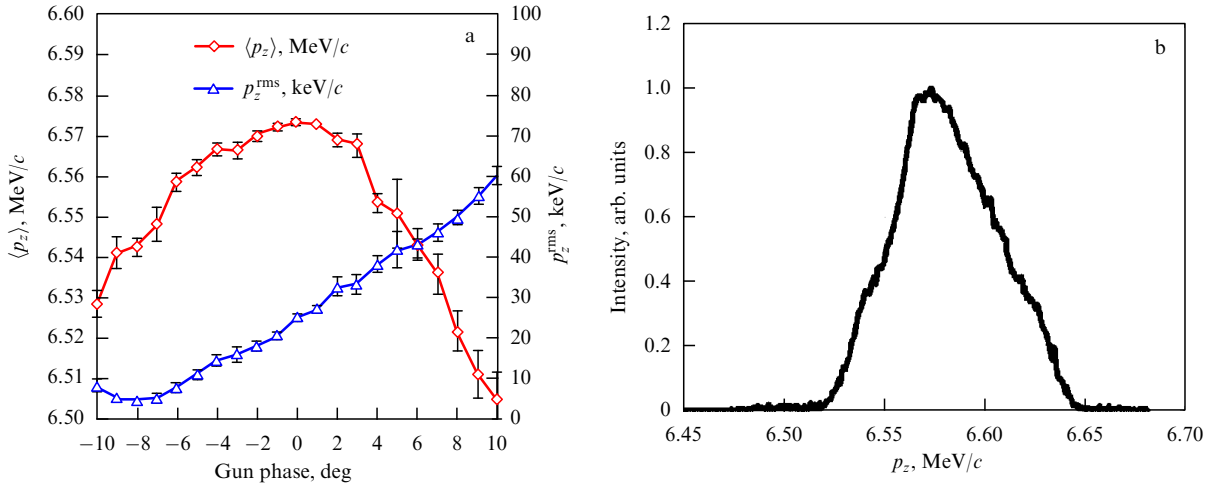

Figure 14. (Color online.) Longitudinal momentum of the electron beam at the gun output: (a) as a function of the microwave gun phase, and (b) projection of the distribution measured for the zero phase of the gun.

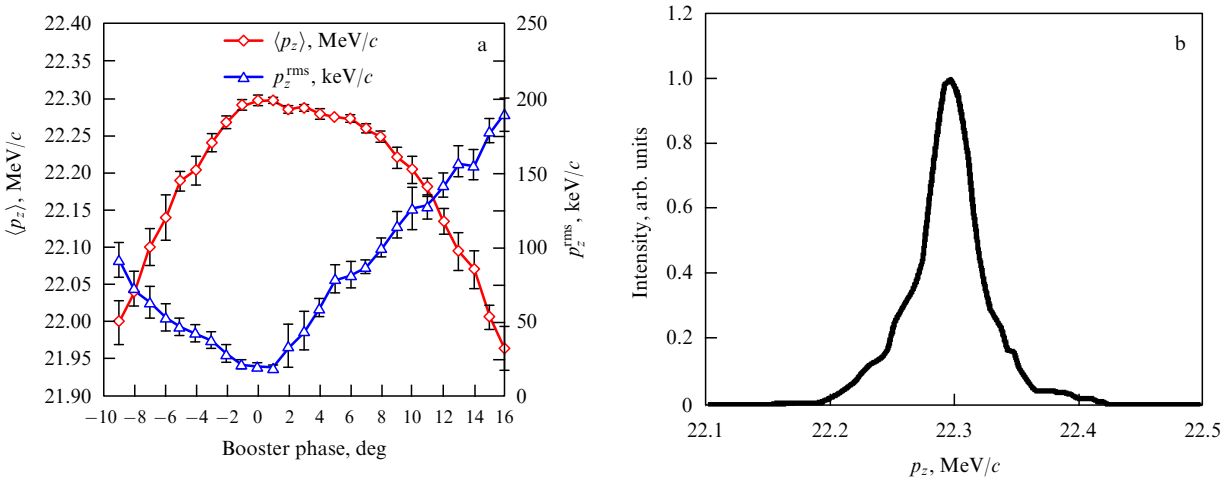

Figure 15. (Color online.) Longitudinal momentum of the electron beam after the booster: (a) as a function of the booster phase, and (b) projection of the distribution measured for the zero phase of the booster. Gun phase was set to zero for all the measurements.

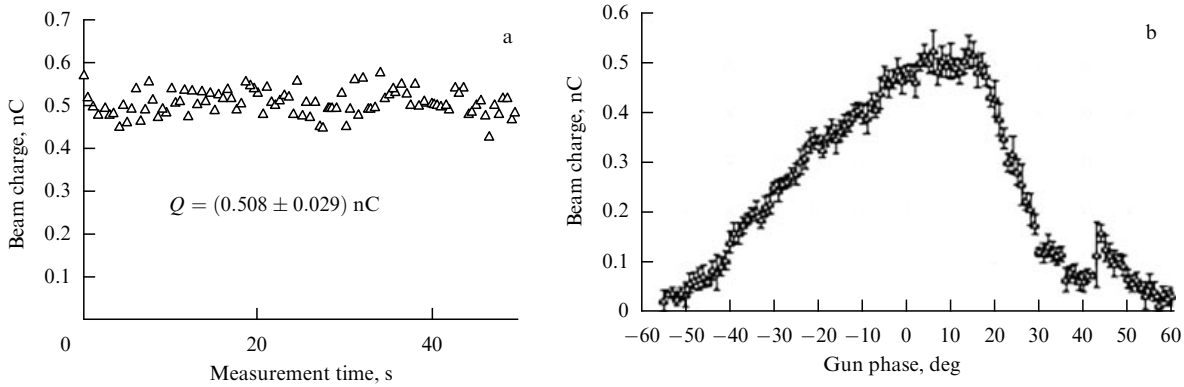

Figure 16. Measured beam charge: (a) for the gun zero phase, and (b) as a function of the gun phase.

from the measured phase dependence that the chosen photoinjector regime demonstrates the large forces of the beam spatial charge, which was also confirmed by measurements of the electron bunch lengths.

Measurement of the transverse emittance dependence on the main solenoid current was performed using a standard for the PITZ method — scanning with a 10-micrometer tungsten slit. As in the previous measurements, the laser beam was restricted by an aperture 1.2 mm in diameter. Measurement results are given in Fig. 17, where the transverse normalized emittance is shown together with beam lateral dimensions measured on an yttrium–aluminum garnet (YAG) scintillat-

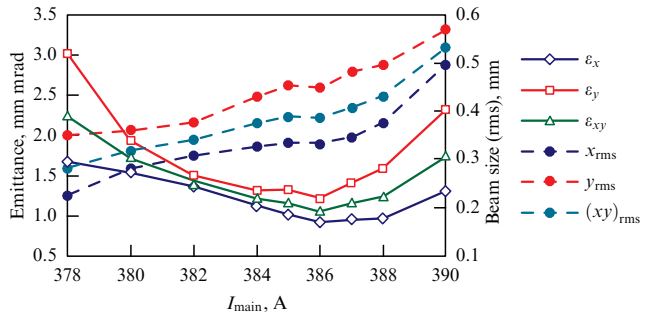

Figure 17. (Color online.) Transverse emittance and root-mean-square lateral size of the electron beam, measured as functions of the main solenoid current.

ing screen at the point where the emittance was measured. Values of the beam size $(xy)_{rms}$ and the emittance ε_{xy} shown in Fig. 17 are the geometric mean values of corresponding vertical and horizontal dimensions.

The transverse distribution of the electron beam and horizontal and vertical phase spaces are shown in Fig. 18 for an optimal solenoid current of 386 A. Corresponding measured values of the emittance are as follows: $\varepsilon_{n,x} = 0.93$ mm mrad, $\varepsilon_{n,y} = 1.22$ mm mrad, and $\varepsilon_{n,xy} = \sqrt{\varepsilon_{n,x}\,\varepsilon_{n,y}} = 1.06$ mm mrad.

The temporal (longitudinal) profile of electron beams with a 0.5-nC charge was measured using a transverse deflecting structure (TDS). The current profile of an electron bunch is plotted in Fig. 19a. Figure 19b shows the density distribution of a deflected beam on the first screen after the TDS. The vertical axis in Fig. 19b is calibrated in picoseconds, in compliance with the TDS phase (2.998 GHz resonance frequency), and is consistent with the horizontal axis scale in Fig. 19a. The measured length of the electron bunch is 15.2 ± 0.5 ps. Similar measurements for the 0.22-nC charge showed a significant decrease in the electron bunch length to 8.2 ± 0.8 ps. This is one more direct evidence of the significant influence of the beam spatial charge on its length, especially in the photocathode region, where the beam energy is quite small.

5. Conclusion

By using a laser system developed at IAP RAS for the PITZ photoinjector, we produced electron bunches with a 0.5-nC charge and 1.1-mm mrad transverse emittance. The laser system allows controling the spatio–temporal distribution of the laser pulse intensity. We have described methods for the formation of 3D ellipsoidal pulses using programmable SLMs and a profiled, chirped volume Bragg grating. Implementation of these methods in the laser system employed for the generation of electron bunches escaping from a photocathode surface will result in a significant decrease in the electron beam transverse emittance.

Acknowledgments

The work was performed in the framework of state assignment of the Russian Federation No. 0035-2014-0016 and with

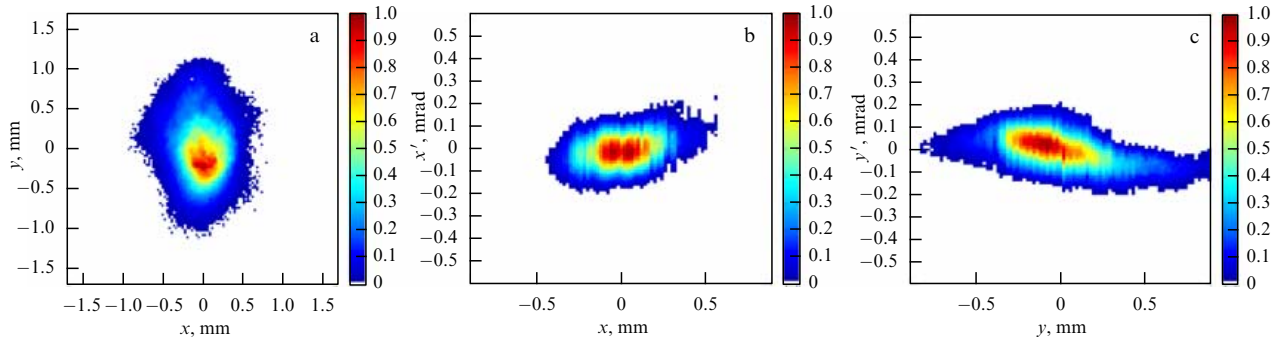

Figure 18. (Color online.) Experimentally optimized emittance: (a) transverse distribution of the electron beam on a scintillating screen, (b) horizontal phase space, and (c) vertical phase space.

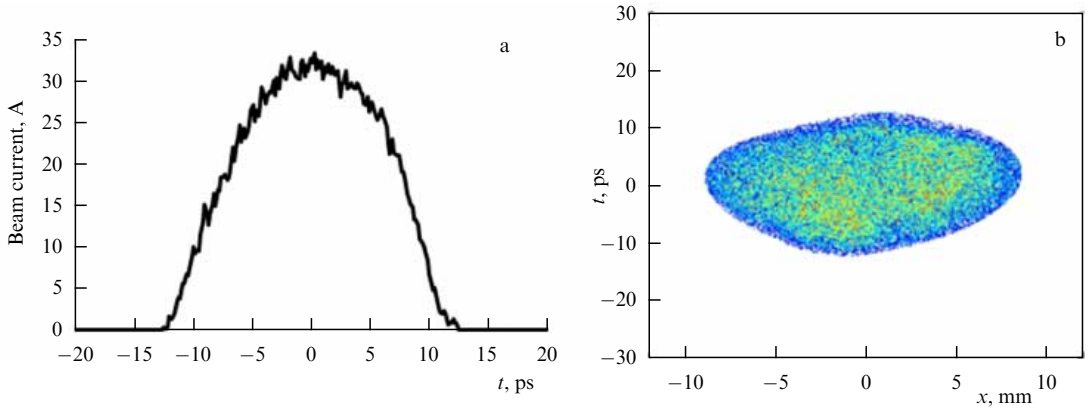

Figure 19. (Color online.) (a) Longitudinal profile of the electron beam — bunch current distribution. (b) Measured shape of the bunch — density distribution of an electron beam deflected in the vertical direction.

the support of the Ministry of Education and Science of the Russian Federation (contract 14.Z50.31.0007).

The authors thank G Asova (Institute for Nuclear Research and Nuclear Power Engineering of the Bulgarian Academy of Sciences, INRNE-BAS) (Sophia, Bulgaria), G Amatuni, N Ghazaryan, B Grigoryan, L Hakobyan, and their colleagues at the Center for the Advancement of Natural Discoveries Using Light Emission (Yerevan, Armenia), who took part in the assembly of the new laser system at the PITZ linear accelerator.

References

1. Interim Report of the Scientific and Technical Issues (XFEL-STI) Working Group on a European XFEL Facility in Hamburg (Hamburg: DESY, 2005)
2. Will I, Klemz G *Opt. Express* **16** 14922 (2008)
3. Krasilnikov M et al. *Phys. Rev. ST Accel. Beams* **15** 100701 (2012)
4. Kapchinskij I M, Vladimirskij V V, in *Proc. of 2nd Conf. on High Energy Accelerators and Instrumentation, 14 - 19 September, CERN, Geneva, 1959* (Ed. L Kowarski) (Geneva: CERN, 1959) p. 274
5. Li Y, Chemerisov S, Lewellen J *Phys. Rev. ST Accel. Beams* **12** 020702 (2009)
6. Musumeci P et al. *Phys. Rev. Lett.* **100** 244801 (2008)
7. Akhmanov S A, Vysloukh V A, Chirkin A S *Optics of Femtosecond Laser Pulses* (New York: AIP, 1992); Translated from Russian: *Optika Femtosekundnykh Lazernykh Impul'sov* (Moscow: Nauka, 1988) p. 41
8. Mironov S Yu et al. *Appl. Opt.* **55** 1630 (2016)
9. Mironov S Yu et al. *Laser Phys. Lett.* **13** 055003 (2016)
10. ASTRA particle tracking code, http://www.desy.de/~mpyflo/
11. Zelenogorskii V V et al. *Quantum Electron.* **44** 76 (2014); *Kvantovaya Elektron.* **44** 76 (2014)
12. Gacheva E I et al. *Opt. Express* **23** 9627 (2015)
13. Efimov O M et al. *Appl. Opt.* **38** 619 (1999)